Received: 15 March 2019 | Revised: 6 June 2019 | Accepted: 4 July 2019

DOI: 10.1002/dvdy.90

RESEARCH ARTICLE

Developmental Dynamics WILEY

Peramorphosis, an evolutionary developmental mechanism in neotropical bat skull diversity

Jasmin Camacho[1] | **Alexander Heyde**[1] | **Bhart-Anjan S. Bhullar**[1,2] | **Danny Haelewaters**[1] | **Nancy B. Simmons**[3] | **Arhat Abzhanov**[1]

[1]Department of Organismic and Evolutionary Biology, Harvard University, Cambridge, Massachusetts

[2]Department of Geology and Geophysics, Yale Peabody Museum of Natural History, Yale University, New Haven, Connecticut

[3]Department of Mammalogy, Division of Vertebrate Zoology, American Museum of Natural History, New York, New York

Correspondence
Jasmin Camacho and Arhat Abzhanov, Department of Organismic and Evolutionary Biology, Harvard University, Cambridge, MA 02138.
Email: jcamacho@fas.harvard.edu (J. C.) and a.abzhanov@imperial.ac.uk (A. A.)

Present address
Arhat Abzhanov, Department of Life Sciences, Imperial College London, Silwood Park Campus Buckhurst Road, Ascot, Berkshire SL5 7PY, UK; Natural History Museum, Cromwell Road, London SW7 5BD, UK.

Danny Haelewaters, Faculty of Science, University of South Bohemia, Branišovská 31, 37005 České Budějovice, Czech Republic.

Funding information
John Templeton Foundation, Grant/Award Number: RFP-12-01; National Science Foundation, Grant/Award Numbers: 1541959, DEB1501690, DGE1144152, IOS-1257122

Abstract

Background: The neotropical leaf-nosed bats (Chiroptera, Phyllostomidae) are an ecologically diverse group of mammals with distinctive morphological adaptations associated with specialized modes of feeding. The dramatic skull shape changes between related species result from changes in the craniofacial development process, which brings into focus the nature of the underlying evolutionary developmental processes.

Results: In this study, we use three-dimensional geometric morphometrics to describe, quantify, and compare morphological modifications unfolding during evolution and development of phyllostomid bats. We examine how changes in development of the cranium may contribute to the evolution of the bat craniofacial skeleton. Comparisons of ontogenetic trajectories to evolutionary trajectories reveal two separate evolutionary developmental growth processes contributing to modifications in skull morphogenesis: acceleration and hypermorphosis.

Conclusion: These findings are consistent with a role for peramorphosis, a form of heterochrony, in the evolution of bat dietary specialists.

KEYWORDS

craniofacial, evo-devo, heterochrony, microCT, peramorphosis, phyllostomidae, skull, three-dimensional geometric morphometrics

1 | INTRODUCTION

"The structure and habits of a bat" puzzled Darwin well over a century ago,[1] yet the subject of the origins and evolution of bats, which as a group represent more than 20% of all mammalian diversity, remains largely under investigated.[2,3] One of the major challenges to understanding bat evolution is the quantitative evaluation of morphological disparity in extant taxa and the lack of fossils needed to trace evolutionary modifications. Within the order Chiroptera, the New

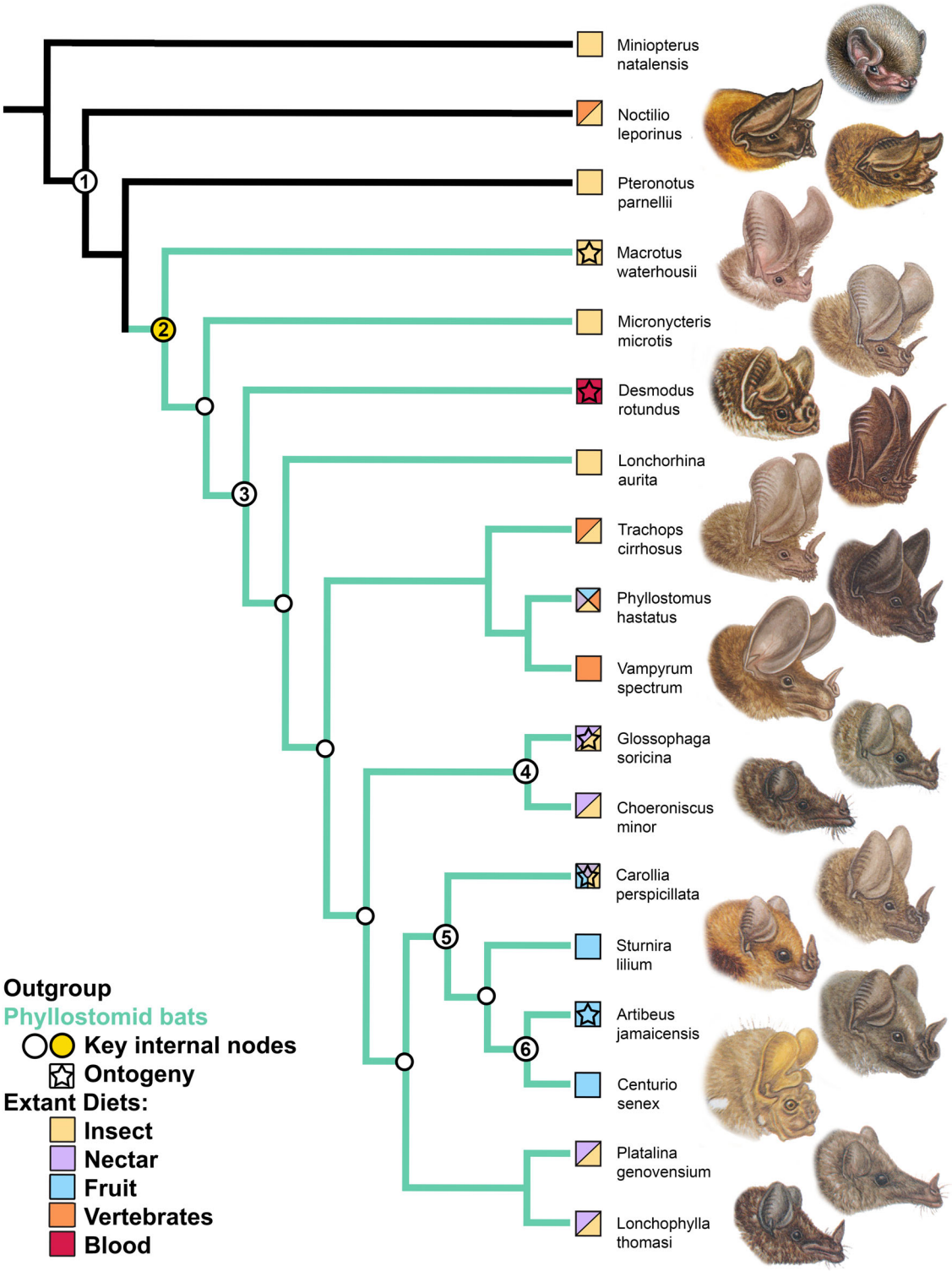

FIGURE 1 Phylogeny and skull diversity in New World leaf-nosed bats (Phyllostomidae). A simplified phylogenetic hypothesis used in this study, rooted using Miniopteridae. Extant taxa (outgroup, black color; phyllostomids, green color) represent the range of ecological and morphological specializations in the superfamily Noctilionoidea. Key internal nodes relative to the origin and diversification: 1, MRCA of neotropical bats; 2, MRCA of phyllostomids; 3, MRCA of vampire bats; 4, MRCA of nectar bats; 5, MRCA of fruit bats; and 6, MRCA of short-face bats. The distribution of feeding habit is indicated by colored boxes, and the ontogenies are indicated by stars. Drawings of bats (courtesy of Fiona Reid) depict the variation in head morphologies of selected skull shapes. MRCA, most recent common ancestor

World leaf-nosed bats (Phyllostomidae) have been extensively studied for their ecology, anatomy, and phylogeny,[4-12] making them an exceptional model for examining mechanisms underlying morphological diversification. As a group, they have evolved an extraordinary array of distinct faces and skulls (Figure 1) adapted for consuming many different food types such as insects, fruit, nectar, pollen, small vertebrates, and blood.[13-17] In this regard, they represent striking examples of adaptions that emerged in response to intense natural selection, similar to Darwin's finches from the Galapagos where beak shapes have adapted to many different food sources.[18]

Previous studies on the morphological evolution in phyllostomids have included reports on biomechanical properties of their diverse skull shapes, such as the relationship of cranial morphology to the bite force[16,17,19,20] or its ability to dissipate mechanical stress.[13,14,21,22] Although functional morphology and feeding ecology provide important insights into skull shape adaptations, they do not explain how the ancestral variation was generated in the first place. To gain such insight, studying morphogenetic developmental processes controlling anatomy is key to understand the origins of morphological diversification, not just for phyllostomid bats but also for any group of multicellular organisms.[23]

In recent years, morphometric studies on cranial shape and comparative investigations of developmental processes have been combined to understand cranial evolution in many vertebrate lineages.[24-30] This allowed for a more detailed and mechanistic understanding of the observed evolutionary diversity patterns.[23,31,32] These types of studies often revealed heterochrony, a change in the timing or order of ancestral developmental events, as an important mechanism for producing evolutionary changes in morphology,[33,34] resulting in hypermature descendants (peramorphosis) or juvenilized (paedomorphosis) versions of their ancestor.[24,35-37] However, no studies to date on phyllostomid evolution have investigated ontogenetic information within a phylogenetic context.

Here, we present the first three-dimensional (3D) geometric morphometric (GM) analysis of skull shape patterns in evolution and skeletal development to determine the mechanism of cranial evolution in phyllostomid bats. We hypothesize that adaptions of phyllostomid bats resulted from widespread peramorphosis by either an increased growth rate or the addition of further ontogenetic steps during evolution. This hypothesis is based on empirical observations on the natural history of phyllostomids, which reveal features that satisfy some of the conditions required for evolution by peramorphosis.[38] First, the basal-most divergences within phyllostomids retain the ancestral insect-feeding diets.[4,13] Second, the features of many derived phyllostomid bats tend to be exaggerated: for example, the leaf-nose is an elaborated rhinarium[39]; vampire bats have relatively large incisors, brains, and eyes[40]; nectar bats proportionally have some of the longest faces and tongues in mammals[41]; and the largest neotropical bat is the phyllostomid carnivore *Vampyrum spectrum*.[42] Most strikingly, compared with other bats, some phyllostomids have an extended gestation period and are born precocial and/or well-furred.[43-48]

To verify the peramorphosis hypothesis, we expect to find that: (a) extant basal lineages will more closely resemble the ancestral state than the more derived lineages; (b) ancestral features will be observed in the early development of all species; (c) species-specific modifications are added after ancestral shape is observed toward the terminal stages of development (terminal addition); (d) ontogenetic and phylogenetic trajectories will be similar in extent and direction of evolutionary change; and the developmental growth rate will be either (d[i]) unchanged (hypermorphosis) or (d[ii]) positive (acceleration).[35,38,49,50]

Our data reveal that embryonic cranial shapes at the stages undergoing early skeletogenesis are geometrically identical to the most recent common ancestor (MRCA) of phyllostomid bats. We also show that ontogenetic trajectories of skull morphogenesis closely coincide with phylogenetic trajectories of their cranial shapes. In addition, we demonstrate that the unique feeding features of phyllostomid bats evolved via peramorphosis by accelerating growth changes (evolution by acceleration) and extending the overall length of gestation (evolution by hypermorphosis).

2 | RESULTS

2.1 | Skull shape evolution

Craniofacial diversity within phyllostomids as a group (Figure 2) appears to be characterized by variations along phylogenetic principal component 1 (pPC1; 69.34%) and pPC2 (27.87%). All other pPCs each describe negligible (<5%) amounts of variation; therefore, we focus our analysis on pPC1 and pPC2. A permutation test (10 000 iterations) failed to identify significant phylogenetic signal in cranial shape variation ($K = 1.16038$, $P = .0386$) and size variation ($K = 0.75353$, $P > .5$). The primary axis of variation describes changes in craniofacial length, width, and height, whereas the second axis of variation represents differences between the cranial profile of leaf-nosed bats from the remaining non-phyllostomid clades, such as *Pteronotus parnellii* (Figure 2). The details of morphological transformations associated with oral and nasal echolocation are described by pPC1 and pPC2 highlighted in Figure 3 by leaf-nosed bat *M. waterhoussii* and outgroup species *P. parnellii*.

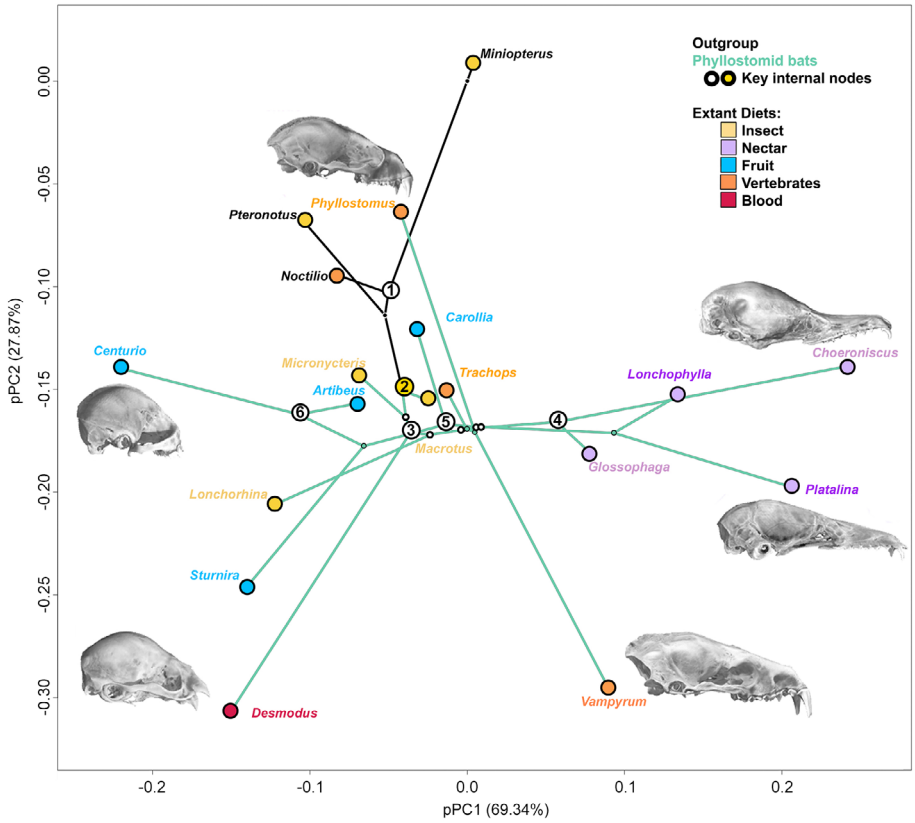

FIGURE 2 Origin and diversification of skull morphology. Phylogenetic phylomorphospace to visualize the extent and direction of evolutionary change along the first two PCs, with ancestral state imputed using maximum likelihood. In general, phyllostomids occupy positions in PC2 morphospace that are distinct from outgroups. The lines connecting species position represent phylogeny. Terminal nodes are colored by diet. Ancestral nodes are colored and labeled as in Figure 1. The three-dimensional μCT images in the skull of adults demonstrate the extreme morphological variability of sampled phyllostomid specimens. Clockwise from top: *Phyllostomus hastatus* (MCZ 27840), *Choeroniscus minor* (AMNH 266124), *Platalina genovensium* (MCZ 32948), *Vampyrum spectrum* (AMNH MS7435), *Desmodus rotundus* (MCZ 47901), and *Centurio senex* (AMNH 175651). μCT, micro-computed tomography; PC, principal component

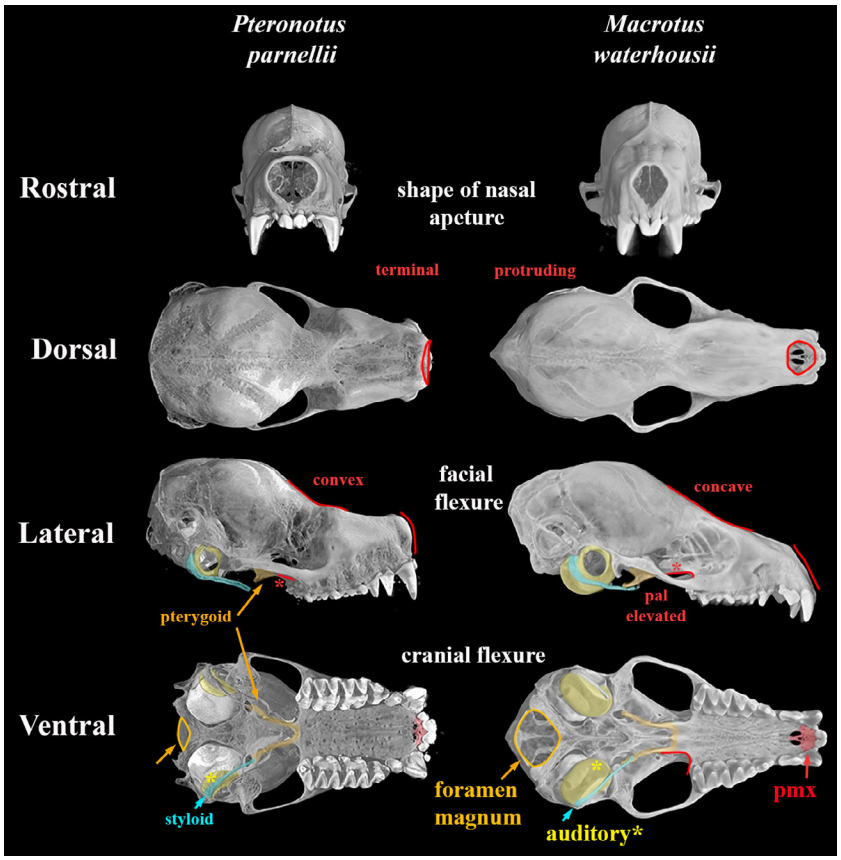

FIGURE 3 Morphological evolution in Chiroptera. Cranial features referred to in the text are highlighted and labeled on the skulls of *Pteronotus parnellii* (Mormoopidae) and *Macrotus waterhousii* (Phyllostomidae, AMNH 204484). *P. parnellii* retains that ancestral oral-emission of echolocation, and *M. waterhousii* has the derived nasal-emission of sound for echolocation. The bat cranium is characterized by five features of particular interest here: the shape of the nasal aperture may be round (top, left) or diamond shape (top, right), the length of the snout may be shortened (top, left) or elongated (top, right), facial flexure may be upturned/convex/airorhynchy (lateral left) or downturned/concave/clinorhynchy (lateral right), cranial flexure may be observed as variation in the position of the foramen magnum relative to the palate (ventral view), and auditory bullae may be enlarged by cochlea (lateral and ventral view, left) or enlarged by the tympanic (lateral and ventral view, right), and the premaxilla may be enlarged (ventral view, right) or reduced (ventral view, left) resulting in a terminal or protruding tooth row (dorsal view). Asterisk (*) notes the inflated tympanic of the auditory bullae

Within phyllostomids, species with the same diet tend to cluster together along pPC1, with fruit- and nectar-eating bats found at opposite ends of this axis ($R^2 = 0.44$, $P < .01$, 10 000 iterations). At positive values of pPC1, faces are long, narrow, and diminished in height and the cranial vault is squat and narrow. The two independently evolved nectarivore bat lineages, Glossophaginae and Lonchyphyllinae,[51] converge in elongated skull morphology specialized for nectar feeding.[14] At negative values of pPC1, faces are short, wide, and elevated in height, and the cranial vault is tall and wide, with a particularly wide temporal bone. Within all bats examined, species with different echolocation call emission behaviors (oral vs. nasal) tend to cluster at the opposite ends of pPC2, consistent with previous studies on cranial diversity in bats.[10,19,52,53] At the negative end of pPC2, the lateral profile of the face is concave (clinorhynchy) and the cranial base is flexed down (Figure 3). Toward the positive end of pPC2, the facial profile is convex (airorhynchy; Figure 3), with *Miniopterus natalensis* showing an extreme upward orientation in its snout (Figure 2).

The skull shape of *Macrotus waterhousii* (insectivore), an extant lineage that diverged about 30–35 m.y.a.,[4,12] is near the consensus shape at the center of the PC analysis (PCA) morphospace (Figure 2). Likewise, several clades (*Micronycteris*, *Trachops*, and *Carollia*) reside at the ends of short evolutionary trajectories, which start near the consensus shape. In contrast, the frugivore (*Centurio senex*), omnivore (*Phyllostomus hastatus*), nectarivore (*Choeroniscus minor*), carnivore (*V spectrum*), and sanguivore (*Desmodus rotundus*) reside at the ends of long and distinct evolutionary trajectories in widely separated regions of morphospace. The evolutionary trajectories observed in species within the major dietary groups (Table 1) differ in magnitude of morphometric change (measured in Procrustes distance) as well as in their orientation of change (slope of the regression line) from the MRCA (node 2; Figure 1) to extant morphologies. Procrustes distances (PD) reveal quantitative differences between short-evolutionary trajectories (*Macrotus*, *Artibeus*, and *Carollia*) and highly apomophic ones (*Glossophaga* and *Desmodus*). Phylogenetically derived dietary specialists are found as radiating in five distinct directions from the insectivore MRCA (node 2; Figure 2). The extant basal lineages within phyllostomids (*Macrotus* and *Micronycteris*) more closely resemble the ancestral state morphology than the more derived lineages.

2.2 | Ontogeny in phyllostomid evolution

Ontogenetic morphological variation was analyzed within the framework of the adult phylomorphospace (Figure 4). Embryonic cranial shapes, as described within the dimensions of PC1 (41% variation) and PC2 (17% variation), all cluster near the mean (ancestral) shape position in the phylomorphospace, near the adult skull shapes of the basal insectivorous *Macrotus* and *Micryonycteris*. This supports another condition for peramorphosis: ancestral features are observed in the early development of all species. The phenotypic changes observed during development, when visualized as a trajectory, closely track phenotypic evolutionary paths in magnitude (Figure 5), an important criterion supporting paramorphosis. The magnitude of shape change (measured in Procrustes distance) from the earliest measured embryonic skulls to the adult shapes is similar for *M. waterhousii*, *Carollia perspicillata*, and *Artibeus jamaicensis*. *Glossophaga soricina* and *Desmodus rotundus* embryos exhibit the greatest magnitude of change from early embryo to adult (PD = 3.81, 6.672). When examining ontogenetic trajectories with common allometric component (CAC)

TABLE 1 Evolutionary and ontogenetic trajectories

Genus	Diet	Procrustes distance	Direction of change	Rate of change	Intercept	R^2	*P* value
Ancestor–descendant							
Desmodus	Blood	63.53	8.216°	0.14438	0.0854	0.8393	.0839
Artibeus	Fruit	0.102	−1.65°	−0.0288	0.1485	0.0023	.9396
Macrotus	Insects	0.02	−5.041°	−0.01504	−0.0199	0.7069	.1592
Carollia	Mix	6.55	−1.117°	−0.01949	0.01771	0.5572	.2536
Glossophaga	Nectar	33.06	−2.869°	−0.05011	0.01533	0.65	.0699
Ancestral proxy-descendant ontogeny							
Desmodus	Blood	66.72	4.415°	0.07720414	0.041042	0.65242	.01
Artibeus	Fruit	0.08	−1.955°	−0.0341304	0.080226	0.63270	.01
Carollia	Mix	5.97	−0.781°	−0.0136312	0.003856	0.62570	.02
Glossophaga	Nectar	33.81	−2.856°	−0.0498944	0.012495	0.50426	.01

Note: Phenotypic evolution of five species across two evolutionary levels (ancestor-descendant), and phenotypic change of five species across development (embryo-adult). Procrustes distance summarizes the extent of evolutionary and ontogenetic shape change. Pairwise Procrustes analysis of variance of trajectories evaluates the direction (arc tangent of the regression line slope), rate of change (slope), and onset of development (intercept).

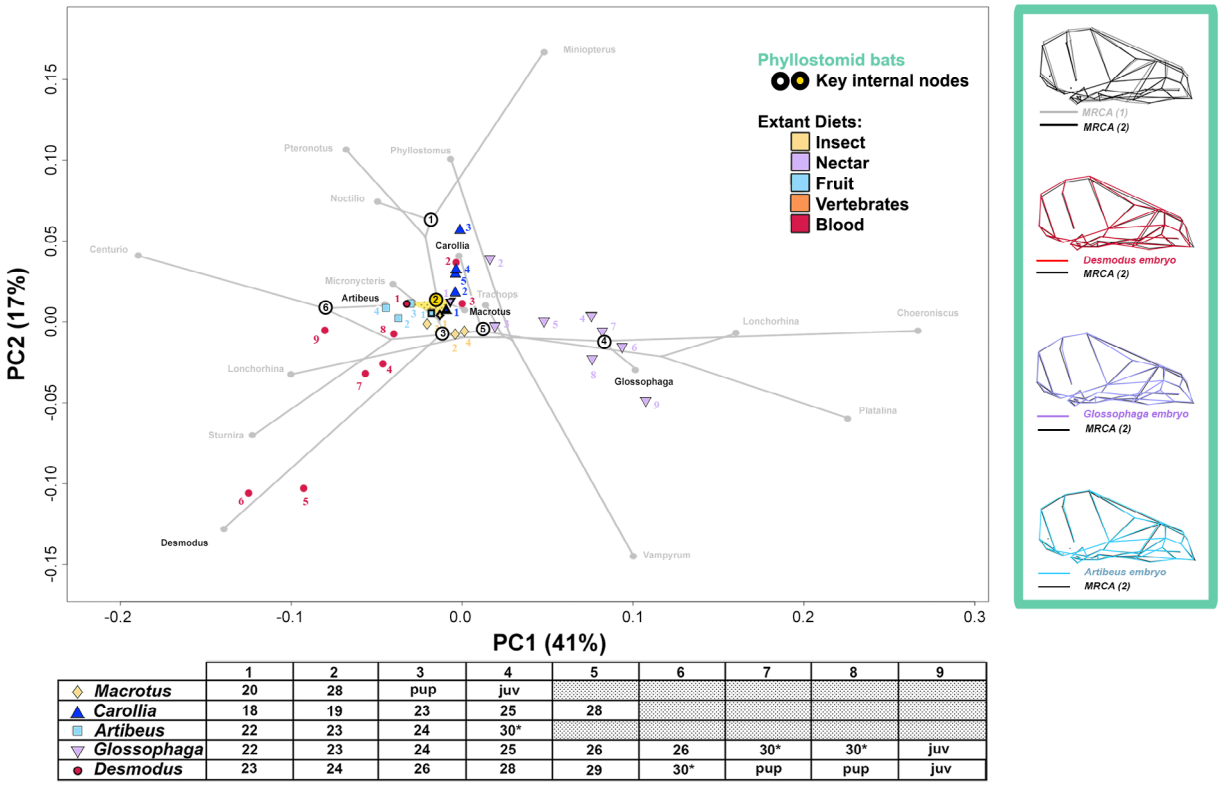

	1	2	3	4	5	6	7	8	9
Macrotus	20	28	pup	juv					
Carollia	18	19	23	25	28				
Artibeus	22	23	24	30*					
Glossophaga	22	23	24	25	26	26	30*	30*	juv
Desmodus	23	24	26	28	29	30*	pup	pup	juv

FIGURE 4 Phenotypic evolution and development. Ontogenetic series for *Macrotus waterhousii*, *Carollia perspicillata*, *Artibeus jamaicensis*, *Glossophaga soricina*, and *Desmodus rotundus* were examined with adults. Early embryos occupy a small region of morphospace (convex hull, yellow dots) and cluster around the reconstructed ancestral shape (MRCA, node 2). Data points are numbered according to stage shown in table below. A generalized "phyllostomid" skull shape is established early in skeletal development (embryo shape 1) and in phyllostomid evolution (MRCA, node 2). The skull wireframes in lateral view demonstrate similar morphology between MRCA to early embryo shape. These diverse species first obtain morphology like the ancestral skull shape before specialized features emerge. PC scores of development closely track the net evolutionary trajectories (thin grey lines) indicated by phylogenetic mapping, demonstrating recapitulation. PC, principal component; MRCA, most recent common ancestor

against cranial size (Figure 6), the nectarivore and sanguivore allometric trajectories followed a similar but more protracted trajectory when compared with that of *Macrotus*, indicating a peramorphic change through hypermorphosis, whereas *Artibeus* and *Carollia* trajectories had a steeper slope compared with the *Macrotus* trajectory, indicating a peramorphism through acceleration.

3 | DISCUSSION

Ancestral features are observed at embryonic stages undergoing early skeletogenesis for all species examined, whereas species-specific and more specialized features are observed toward the terminal stages of development (Figure 4). Comparisons of ontogenetic trajectories between species suggest an overall pattern of heterochrony by peramorphosis (Figure 6). Morphologically highly derived sanguivore *D rotundus* and nectarivore *G soricina* have similar but protracted ontogenetic trajectories compared with the more conservative *M waterhousii*. Comparisons of the patterns of morphological change in evolution and development in phyllostomids reveal an additional feature of their peramorphosis—that most of ontogeny recapitulates evolutionary trends (Figures 4 and 5). Since the period of developmental growth is prolonged (i.e., morphogenetic processes take a longer time to be completed) into postembryonic juvenile development (Table S1), we conclude that the main developmental mechanism for the evolution of vampire and nectar-feeding bats was peramorphosis by hypermorphosis.

Generalist (with *Piper* fruit preference) *C. perspicillata* and frugivore *A. jamaicensis* had ontogenetic trajectories similar to each other in extent and direction of morphological change but displayed steeper ontogenetic slopes compared to *M. waterhousii*, suggesting peramorphosis by acceleration (Figure 6). Closer examination of the species-specific patterns of morphological changes in evolution of these species further supports this conclusion by revealing similar morphological changes in development emerging during comparable growth periods (Figures 4 and 5).[38,49,50] Interestingly, that the *Carollia* lineage is basal to the adaptive radiation of the Stenodermatinae lineage (represented by *Artibeus* in Figure 1) seems to suggest that

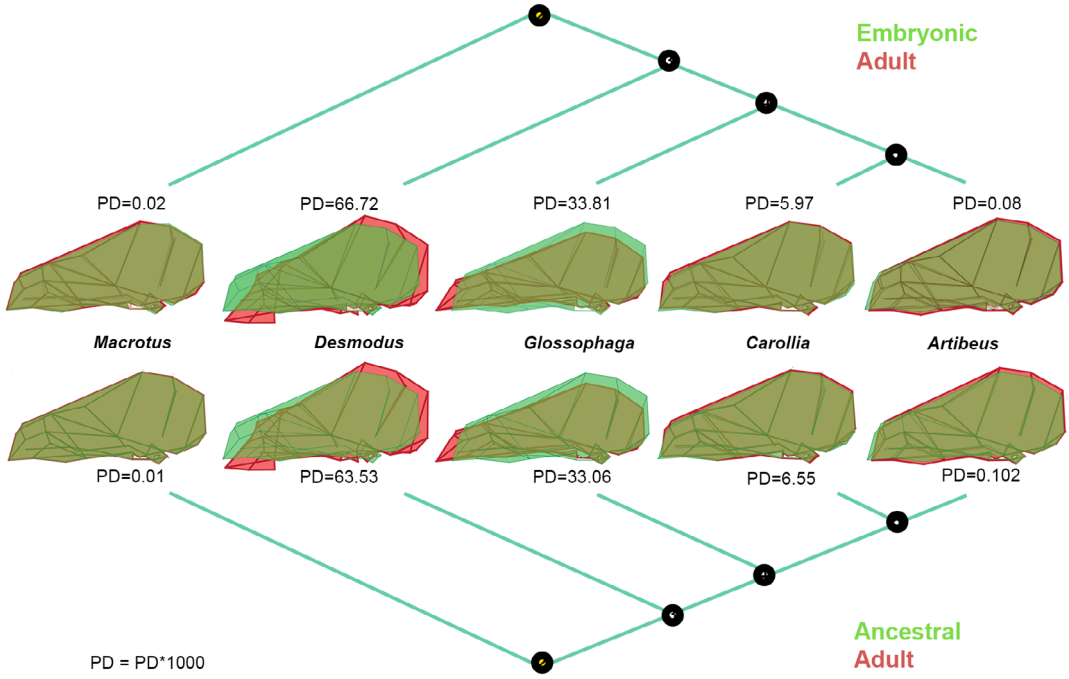

FIGURE 5 Extent of evolutionary and ontogenetic shape change. Wireframes of skull shapes were overlaid to compare patterns across ontogeny and evolution. The overall changes in ontogeny from embryo to adult matched the overall changes from MRCA to adult. *Macrotus waterhousii*, *Carollia perspicillata*, and *Artibeus jamaicensis* deviate slightly from the calculated ancestral skull shape during evolution. *Glossophaga soricina* and *Desmodus rotundus* deviate significantly from the ancestral shape and each other, achieving substantially altered adult shapes. MRCA, most recent common ancestor

peramorphosis has been the most likely ontogenetic modification allowing for rapid diversification in frugivore morphology.

When changes occur at the terminal stages of development by the addition of novel stages not present in the common ancestor, a phenomenon called *terminal addition*,[38] then the length of ontogeny becomes longer and can be classified as hypermorphosis model of heterochrony. If novel stages are added at the terminal stage of development, but the overall duration of shape change is unaffected, then each developmental stage (recognized as shape change) proceeds more quickly. Terminal addition with an increase in the rate of developmental changes can then be also described as the acceleration model of heterochrony. Hypermorphosis and acceleration can occur at any point in development, but we observed that the cranial shape changes during bat ontogeny are restricted only to the terminal stages of development, more in agreement with the terminal addition scenario. We noted that terminal addition manifests itself as a recapitulation, when ontogeny of cranial shape changes matches their evolutionary trends. This model of evolution predicts that fossils will be found representing more or less linear transitions from the ancestral insectivorous shape and towards each of the more derived and specialized conditions. This prediction is supported by the oldest fossil nectar bat *Palynephyllum antimaster*.[54] The authors estimated that the extinct bat ate a mix of both insects and nectar prior to the highly specialized nectar-only diet in the extant lonchophylline species. It is likely other fossils (such as preserved molar teeth) relevant to phyllostomids will have signatures of an omnivorous transition prior to diet specialization, as in this case a single molar tooth of *P antimaster* was sufficient to infer both its phylogenetic relationship and its diet.[55] However, *P. antimaster* remains thus far the only existing case study supporting our hypothesis and more fossils are needed.

Evolution by terminal addition is a relatively rare phenomenon, as this relationship can be easily and quickly obscured by other forms of heterochrony.[38,56,57] However, recapitulation through terminal addition does occur and, as our observations suggest, may in fact be widespread within some recent vertebrate radiations. Studies on relatively recent adaptive morphological radiations (1–20 m.y.a.) in diverse clades as disparate as Darwin's finches,[58,59] anole lizards,[32,60] flatfish,[61] and bats[62] all suggest sequential changes in their ontogeny, especially at later embryonic and postembryonic stages, which may be reflective of the recent evolutionary changes within these groups and more generally within vertebrates.[63] The exact molecular mechanisms by which new evolutionary changes are incorporated into the developmental progression are not yet clear, but the

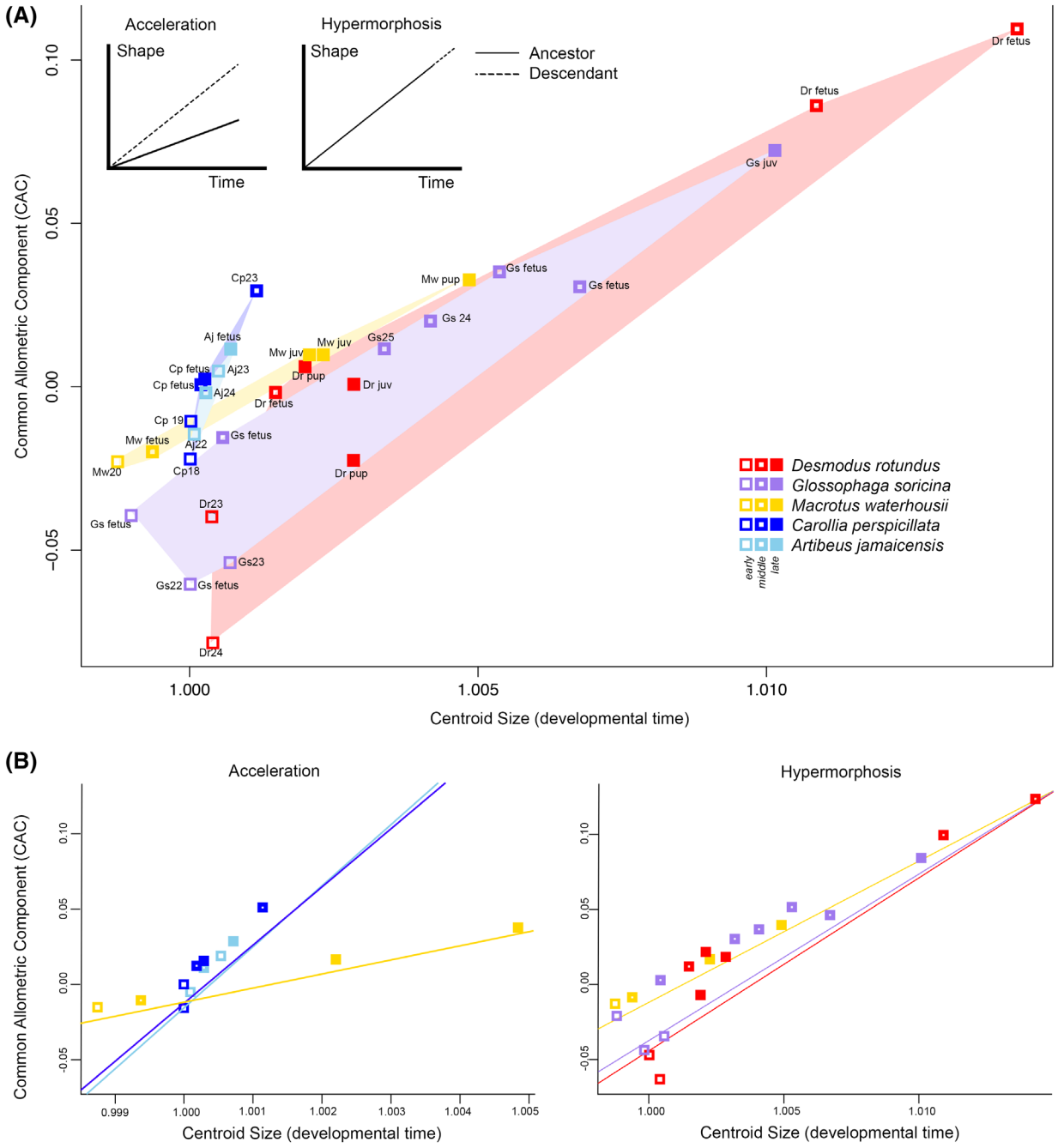

FIGURE 6 Ontogenetic and heterochrony analysis. A, Regression analysis of 3D shape (common allometric component score) onto centroid size during skeletogenesis for *Macrotus* (gold), *Carollia* (dark blue), *Artibeus* (blue), *Glossophaga* (purple), and *Desmodus* (red). *Macrotus* is used as a proxy for ancestral development. The top left shows expected regression lines for the acceleration and hypermorphosis model of heterochrony. B, Ontogenetic trajectories suggesting peramorphosis by acceleration and hypermorphposis. Early (open square), middle (filled square), and late (closed square) stage embryos. 3D, three dimensional

nature of ontogenetic modification by terminal addition likely reflects the intrinsic hierarchy and evolutionary constraints in the developmental process itself.

3.1 | Experimental procedures

To document patterns of evolutionary and developmental changes in phyllostomid cranial adaptive traits, we employed high-resolution micro-X-ray computed tomography (μCT) imaging and 3D landmark-based geometric morphometry,[64] followed by PCA of skull shape variation. Phyllostomid species were selected to capture diversity of feeding, phylogenetic position, morphological variation, and ontogeny. We included representatives of the sister families as outgroups to polarize macroevolutionary changes within phyllostomids.

3.2 | Samples

All geometric morphometric analyses (n = 137) were based on extant specimens from mammalogy collections in the Museum of Comparative Zoology, Harvard University, and the American Museum of Natural History, New York (Table S2). Fifteen species of phyllostomids were sampled at different phylogenetic positions in each major subfamily (Figure 7). Up to 10 specimens were sampled per species when possible (N = 3–10). Species from three related families of bats, *P. parnellii* (n = 3, Family Mormoopidae), *Noctillio leporinus* (n = 5, Family Noctilionidae), and *M. natalensis* (n = 5, Family Miniopteridae) were included as outgroups. Bat species were classified by diet following[67]—(a) insectivorous: insects and arthropods constitute >80% of diet, (b) piscivorous: fish represent >50% of diet, (c) carnivorous: terrestrial vertebrate prey consumed in >60% diet, (d) nectarivorous: nectar and pollen consumed regularly and species has sensory and behavioral specializations to extract nectar from a flower corolla, (e) frugivorous: diet is >70% fruit material, (f) omnivorous: fruit, nectar, and >15% insects consumed or fruit, nectar, insects, and >20% terrestrial vertebrates in natural diet, and (g) sangivourous: diet is >99% blood. Categorizations and cutoffs were based on dietary data and behavioral observations from the literature.[67-76]

Ontogenetic specimens were limited by availability of material (Table S2). Embryonic and fetal specimens were dissected from ethanol-preserved females, and five phyllostomid species were selected for analysis based on the range of available embryonic ages (Figure 1): *M. waterhousii* (insectivore), *C. perspicillata* (omnivore, *Piper* preference), *A. jamaicensis* (frugivore generalist, preference for *Ficus*), *G. soricina* (nectarivore), and *D. rotundus* (sanguivore). All embryo specimens were staged using external morphological features as described in Table S3 and subdivided into three developmental periods based on their degree of skeletal development. Early embryos refer to Carnegie stage (CS) 17–20, mid-embryo age refers to CS21–24, late stages beyond the Carnegie staging system[43] were assigned ascending values, CS25–30, and refer to fetal stages prior to birth. Postnatal bats were not assigned a CS and classified into pups or juveniles according to dentition and sutural fusion.

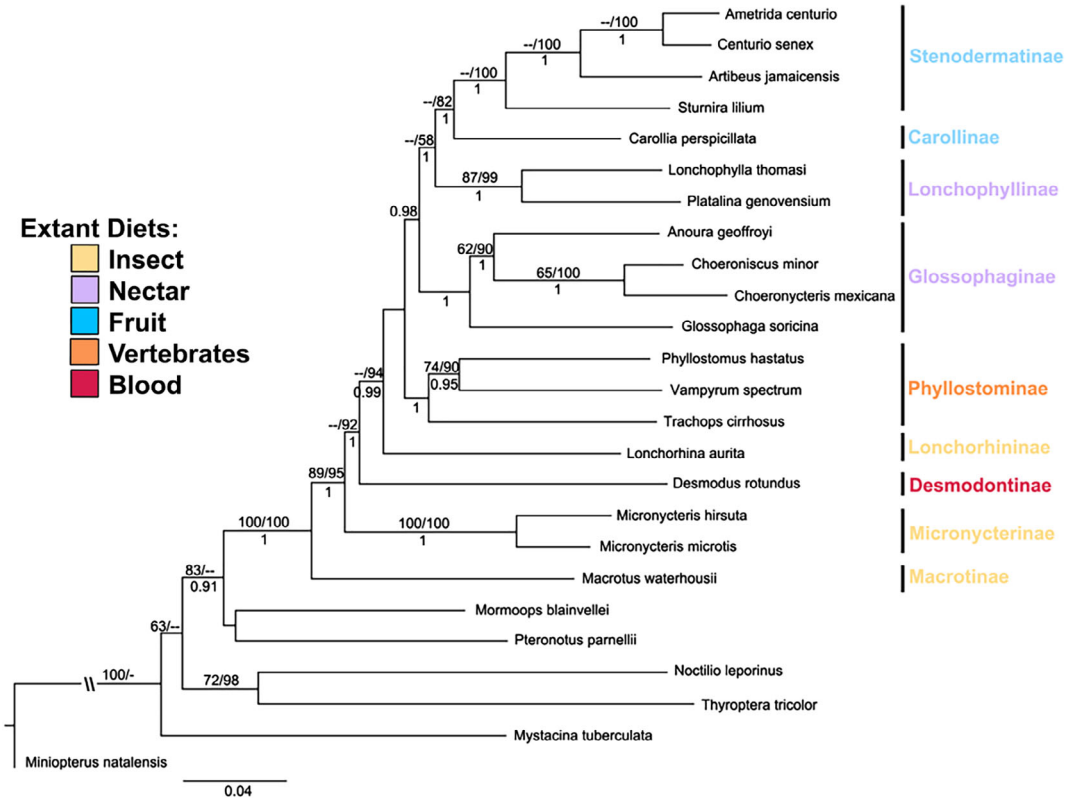

FIGURE 7 Molecular phylogeny. The phylogenetic hypothesis used in this study is a pruned molecular phylogeny of noctilionids, mormoopids, and phyllostomids. The tree was assembled by analyzing nine gene regions (Table S1). *Miniopterus natalensis* was used to root the tree. Our phylogeny is broadly congruent with previously published phylogenies.[4,12,14,65,66] Nine subfamily-level lineages are identified within phyllostomids: Macrotinae, Micronycterinae, Desmodontinae, Lonchorhininae, Phyllostominae, Glossophaginae, Lonchophyllinae, Carollinae, and Stenodermatinae (colored by primary diet similar to Figure 1). MP and ML bootstrap values are indicated (MP/ML) and posterior probabilities (PP > 0.90) are given at each node. MP, maximum parsimony; ML, maximum likelihood

3.3 | X-ray CT

We obtained skull shape data by using nondestructive, high-resolution X-ray μCT. All scans were made with a Nikon HMX-ST-225 μCT machine at the Laboratory for Integrated Science and Engineering, Harvard University, using a molybdenum target that generates low energy X-rays for biological specimens. Embryonic material was scanned individually for early stages and batch-scanned for older stages, with two to four specimens per scan. CT scan data were rendered as 3D volumes using VG Studio Max v2.2–3.0.[77] Bone was segmented from embedding media by applying a threshold for bone, and lower jaws were digitally removed (Figure 8). Details of individual scans are available from the corresponding authors. CT scan data will be deposited to respective museums.

3.4 | Landmark and shape analysis

Cranial shape was characterized by landmark-based GMs.[64] Landmarks were digitized in 3D over the cranium (Figure 8; Table S4), representing anatomically defined points (type I landmarks) using the digital indicator tool in VG Studio Max v2.2–3.0.[77] Type II landmarks, homologous points defined by geometry (e.g., point of maximum curvature), were used to maximize shape information in cranial regions with more intricate shape, such as the ectotympanic. Landmark data were subjected to full Procrustes fit within species to compute group-mean landmark ordination within the MorphoJ software.[78] Species-mean shapes were calculated and extracted from MorphoJ and all phylogenetic and ontogenetic comparative analyses were performed in R.[79]

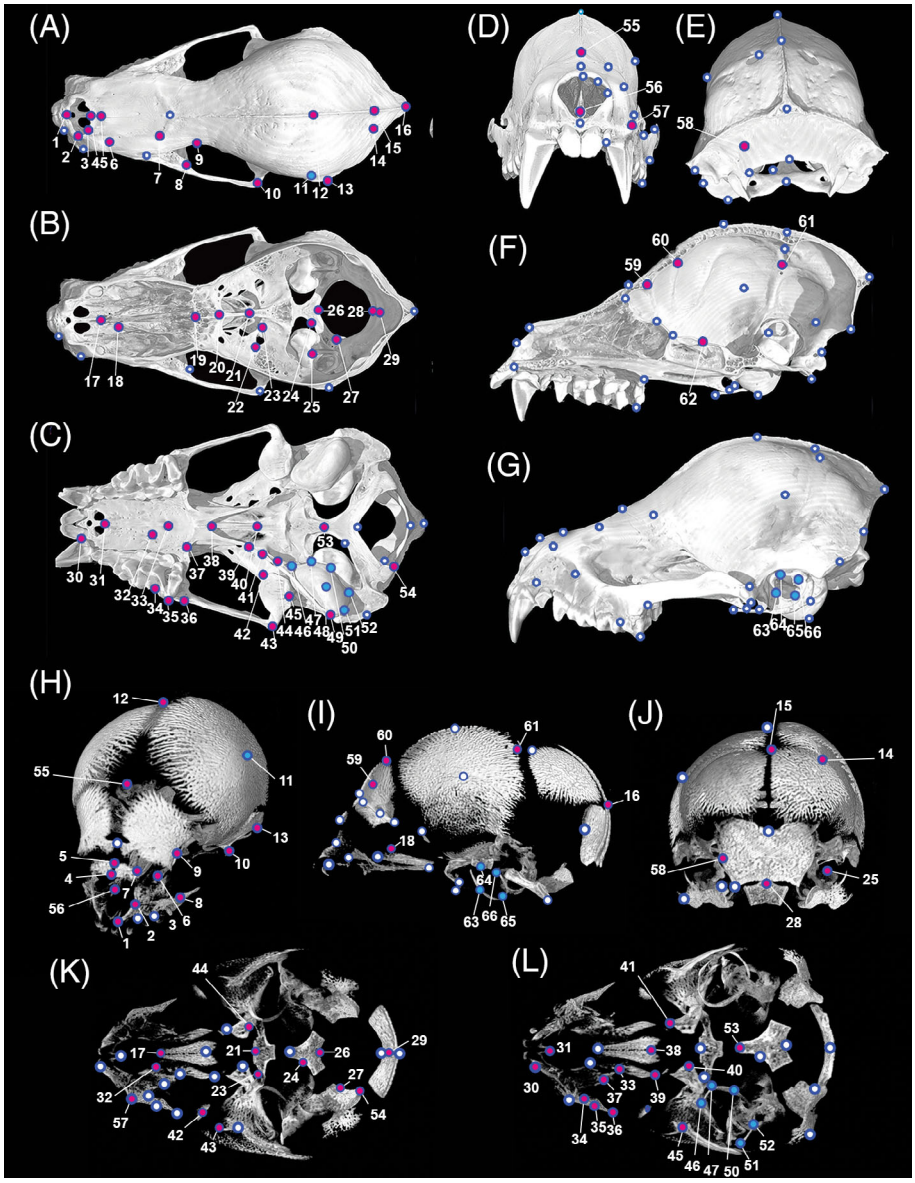

FIGURE 8 Landmarks used in the study to characterize cranial shape and development. Landmarks digitized on skull at dorsal (A, K), internal dorsal (B), ventral (C, L), anterior (D, H), posterior (E, J), parasagittal (F), and lateral (G, I) in adult (A–G) and embryo (H–L). Red circles indicate type I landmarks, blue circles indicate type II landmarks, and white circles indicate landmarks inside the braincase. The three-dimensional microCT image in adult is the skull of *Trachops cirrhosus* (AMNH 266079) and the embryo is the skull of *Desmodus rotundus* (AMNH 203778). Numbers refer to detailed definitions of landmarks in Table S2. microCT, micro-computed tomography

3.5 | Phylogeny

The phylogenetic hypothesis for this study is a topological synthesis constructed from a molecular phylogeny constructed with Markov chain Monte Carlo coalescent approach implemented in BEAST v1.8.4[80] using nuclear and mitochondrial sequences for 19 phyllostomid species and 6 outgroup species (Table S5). The data matrix consisted of 9344 characters, 5831 of which were constant and 2144 were parsimony-informative. The XML file for BEAST was made with BEAUti v1.8.4 by importing the NEXUS file of the combined data matrix. A Bayesian skyline coalescent tree prior was used in four independent runs from a randomly generated starting tree with a chain length of 10 million generations and sampling frequency of 1000. Tracer v1.6[81] was used to check effective sample size (ESS) to achieve a combined ESS >200. TreeAnnotator v1.8.4 was used to generate consensus trees with 0% burnin and to infer the Maximum Clade Credibility tree. A summary of the supporting evidence for each node is given in Figure 7. The molecular phylogeny was pruned to the relevant taxa for morphological analysis (Figure 1). The XML, log, and tree files are available for download from the figshare online repository (doi:10.6084/m9.figshare.c.3892243).

We also performed maximum parsimony (MP) and maximum likelihood (ML) analyses using PAUP* v4.0b10.[82] Maximum parsimony inference with heuristic search consisted of 500 stepwise-addition trees obtained using random sequence addition replicates followed by tree bisection-reconnection (TBR) branch swapping, MulTrees in effect, and saving all equally most parsimonious trees. Robustness of branches was estimated by MP bootstrapping, using 200 bootstrap replicates, with TBR branch swapping, a rearrangement limit of 1000, and MaxTrees set at 100. Maximum likelihood was estimated under a GTR + I + G model of nucleotide substitution, with 1000 bootstrapping replicates.

3.6 | Phylomorphological space

PCA was performed with the Geomorph R package[83] on the total data set (adults and embryos) to quantify variation in skull shape. Phylogenetic signal in size and shape was evaluated with a permutation test with 10 000 iterations with Geomorph.[83] Blomberg's *K* is expected to be equal to 1.0 under Brownian motion. Significant difference from 1.0 is evidence for phylogenetic relationships affecting size and shape values. Phylogenetic PCA was performed with the R package phytools[84] with adult data only. Phylogeny and specimen positions were mapped to the tangent space defined by the first two pPC and illustrate the evolutionary history in morphospace ordination. Internal nodes (ancestral states) were calculated with ML estimation under a Brownian motion model of evolution. Ancestral state coordinates were extracted for subsequent trajectory analysis.

Four key cranial features investigated using this approach are illustrated in Figure 3. First, facial length was captured in width, height, and flexure (landmarks 1, 4, 5, 37, 38, 40, and 55 and paired landmarks 6, 7, 8, 37, and 57 in Figure 8). The nasal septum length and height (landmarks 17, 18, 19, 20, 56, and 38 in Figure 8) are additional internal features that may contribute to facial variation. In addition, variation in cranial vault shape and size is readily visible on dorsal and lateral views (landmarks 5, 12, 15, 16, 21, 26, 29, and 55 and paired landmarks 9, 11, 14, and 58-61 in Figure 8). Second, the size of the nasal aperture (landmarks 1 and 4 and paired landmarks 2 and 3) and its position is described as terminal/protruding (landmark 31 and paired landmarks 30 and 57 in Figure 8). Third, cranial base shape (landmarks 19-24, 26-28, 41, 44, 45, 54, 56, and 62 in Figure 8) and flexure are highlighted by the position of the foramen magnum relative to palate (Figure 3). Fourth, continuous variation in the size, shape, and position of the auditory bullae (paired landmarks 46-52 and 63-66), pterygoids (landmarks 37-41 and 44), and styloid fusion with the tympanic (landmarks 39, 41 and 49) are highlighted with consideration to echolocation.

3.7 | Trajectory analysis

We assessed patterns of morphological evolution using comparisons across two evolutionary levels (ancestral-descendant) and morphological development with comparisons across ontogeny (embryo-adult). Ancestral state coordinates from pPCA for the most recent ancestor common ancestor (2. MRCA) of phyllostomid bats (Figure 1) and internal nodes leading to the origin of sanguivory (3. MRCA), Glossophaginae nectarivory (4. MRCA), frugivory (5. MRCA), and short-faced frugivory (6. MRCA) were used to calculate ancestral trajectories using regression analyses against log transformed centroid size. The extent and direction of morphological trajectory is highlighted by PC1 and PC2 shape variance. Similarly, ontogenetic trajectories were calculated using allometric regressions of Procrustes-aligned coordinates against centroid size.

3.8 | Ontogeny and heterochrony analysis

Conventionally, heterochrony is detected as peramorphosis or pedomorphosis by examining the regression of shape changes onto centroid size.[64,85-87] Average species ontogenetic trajectories in 3D shape were examined with Procrustes ANOVA using the CAC, a vector of regression slopes estimated from Procrustes shape variables,[27] with the *procD.lm* function in the R package Geomorph with 10 000 iterations.

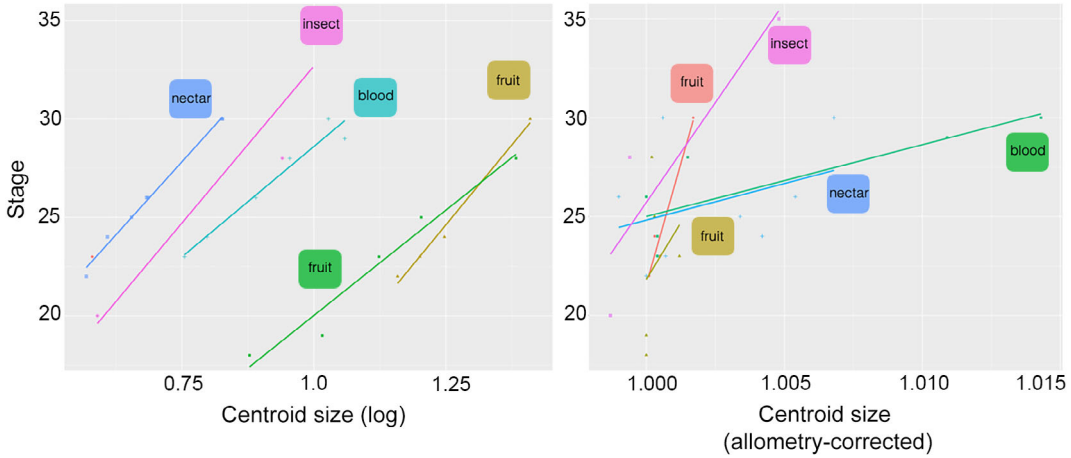

FIGURE 9 Comparing centroid size and stage. Staging of embryos was assigned based on morphological features and independent of size. In statistical shape analysis, size, represented as the log-CS, is commonly used as a proxy for age. CS values within a species relate to stage, but CS values between species do not relate to stage. So, although size is a great proxy for age within a species, the size does not match the equivalent stages among the different species. To compare stage-matched embryos between species, an allometric correction was performed on the shape coordinates, and then the CS of residual shapes was extracted. The allometry-corrected CS was a better proxy for stage. Thus, bats of same stage are scaled to the same size, or normalized. CS, centroid size

CAC is mathematically equivalent to the shape scores from the regression of shape on size.[83] To compare stage-matched embryos between species, an allometric correction was performed on the shape coordinates, then the centroid size of residual shapes was extracted (Figure 9). The allometry-corrected CS was a better proxy for stage (Figure 10). Thus, bats of same stage are scaled to the same size, or normalized.

As *M waterhousii* is the basal-most divergence within phyllostomids and retains an ancestral insect-feeding mode, we use its ontogenetic trajectory as a proxy for the ancestral developmental condition. Procrustes ANOVA was done to assess the relationship between shape and size with the homogeneity of slopes test to determine if species significantly differed in their trajectories, followed by Pairwise Procrustes ANOVA of ontogenetic trajectories (Table 1) to determine how species differed from *Macrotus*. Changes in slope signify changes to the rate of development. Changes in intercept signify changes to the onset of development. All statistical tests were performed on Procrustes-aligned landmark coordinates.

3.9 | Heterochronic shifts

We expect deviations from the ancestral development by heterochrony to lead to different CACs. Different known types of heterochrony include: development beyond the ancestral state (hypermorphosis), development stopping before ancestral condition is reached (progenesis), development starting earlier (predisplacement), development starting later (postdisplacement), and rate of development occurring faster (acceleration) or slower (neoteny). To predict key aspects indicative of heterochronic changes, such as onset/offset, growth rate, and length of development, we examine the relationships between evolutionary and ontogenetic changes in skull shape (extent and direction). The magnitude of phenotypic change in evolution and ontogeny was calculated with PD. We compare PD between adult shapes to the MRCA and early embryo shape to their respective adult shape. We compare evolutionary and ontogenetic trajectories by slope and intercept.

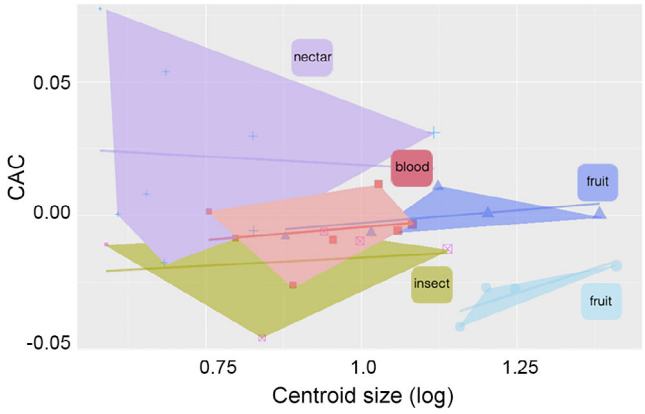

FIGURE 10 Log centroid size and shape prior to allometric correction. Heterochrony is detected by regression of shape onto the log centroid size. Compared with the trajectory of *Macrotus*, an insect-feeding bat, fruit bat trajectories have steeper slopes, a signature of acceleration. Compared with the trajectory of *Macrotus*, blood- and nectar-feeding bats have similar slopes but differ in the extent of shape change, a signature of hypermorphosis. The convex hulls capture the extent of shape variation during ontogeny. CAC, common allometric component

AUTHOR CONTRIBUTIONS

A.A. and J.C. designed the study. J.C. and A.H. performed CT scans, data entry, analytical work, and figures. J.C., N.B.S., and B.-A.S.B. performed morphological data interpretation. D.H. performed phylogenetic analyses. J.C., A.H., A.A., and N.B.S. cowrote the article.

ACKNOWLEDGMENTS

We thank F. Kosar for imaging assistance, Zachary Morris and Drs. J. B. Losos, C. T. Tabin, J. Hanken, and A. Soto-Centeno for comments that substantially improved the article, and Judy Chupasko and Mark Omura of the Museum of Comparative Zoology at Harvard University and staff at the American Museum of Natural History in New York for curatorial support. D. Haelewaters thanks the Graduate School of Arts and Sciences at Harvard University for providing the funds to attend the Workshop on Molecular Evolution at Woods Hole (2013). Any opinions, findings, and conclusions or recommendations expressed in this material are those of the authors and do not necessarily reflect the views of the NSF.

ORCID

Jasmin Camacho https://orcid.org/0000-0001-6449-9224
Danny Haelewaters https://orcid.org/0000-0002-6424-0834
Arhat Abzhanov https://orcid.org/0000-0002-9147-0168

REFERENCES

1. Darwin C. *On the Origin of the Species*. London, England: Routledge; Vol 5; 1859:386.
2. Gunnell GF, Simmons NB. *Evolutionary History of Bats: Fossils, Molecules and Morphology*. Cambridge Studies in Morphology and Molecules: New Paradigms in Evolutionary Bio. New York, NY: Cambridge University Press; Vol 94; 2012:105-161.
3. Simmons NB. Chiroptera. *Mammal Species of the World: A Taxonomic and Geographic Reference*. Baltimore, MD: JHU Press; Vol 1; 2005:312-529.
4. Baker RJ, Olaf R, Bininda-Emonds HM-M, Calvin A, Van Den Bussche R. Molecular timescale of diversification of feeding strategy and morphology in New World leaf-nosed bats (Phyllostomidae): a phylogenetic perspective. In: Gunnell GF, Simmons NB, eds. *Evolutionary History of Bats: Fossils, Molecules and Morphology*. New York, NY: Cambridge University Press; 2012:385-409.
5. Baker RJ, Hoofer SR, Porter CA, Van den Bussche RA. *Diversification among New World Leaf-Nosed Bats: An Evolutionary Hypothesis and Classification Inferred from Digenomic Congruence of DNA Sequence*. Lubbock, TX: Natural Science Research Laboratory; *Occasional Papers, Museum of Texas Tech University*; 2003:1-32.
6. Dávalos LM. Earth history and the evolution of Caribbean bats. In: Fleming TH, Racey PA, eds. *Island Bats: Evolution, Ecology, and Conservation*; Chicago, IL: University of Chicago Press; 2010:96-115.
7. Ferrarezzi H, Gimenez EDA. Systematic patterns and the evolution of feeding habits in Chiroptera. *J Comput Biol*. 1996;1:75-94.
8. Freeman PW. Macroevolution in microchiroptera: recoupling morphology and ecology with phylogeny. Mammalogy Papers: University of Nebraska State Museum; 2000:8.
9. Gardner AL. Feeding habits. In: Jones K, Carter DC, Baker RJ, eds. *Biology of Bats of the New World Family Phyllostomatidae. Part II*. Lubbok, TX: Texas Tech Press; 1977:293-350.
10. Pedersen SC. Cephalometric correlates of echolocation in the Chiroptera. *J Morphol*. 1993;218:85-98.
11. Sadier A, Davies KT, Yohe LR, et al. Multifactorial processes underlie parallel opsin loss in neotropical bats. *Elife*. 2018;7:e37412.
12. Shi JJ, Rabosky DL. Speciation dynamics during the global radiation of extant bats. *Evolution (N. Y.)*. 2015;69:1528-1545.
13. Dumont ER, Davalos LM, Goldberg A, Santana SE, Rex K, Voigt CC. Morphological innovation, diversification and invasion of a new adaptive zone. *Proc R Soc B Biol Sci*. 2012;279:1797-1805.
14. Dumont ER, Samadevam K, Grosse I, Warsi OM, Baird B, Davalos LM. Selection for mechanical advantage underlies multiple cranial optima in new world leaf-nosed bats. *Evolution (N. Y.)*. 2014;68:1436-1449.
15. Harper CJ, Swartz SM, Brainerd EL. Specialized bat tongue is a hemodynamic nectar mop. *Proc Natl Acad Sci U S A*. 2013;110:8852-8857.
16. Nogueira MR, Peracchi AL, Monteiro LR. Morphological correlates of bite force and diet in the skull and mandible of phyllostomid bats. *Funct Ecol*. 2009;23:715-723.
17. Santana SE, Dumont ER, Davis JL. Mechanics of bite force production and its relationship to diet in bats. *Funct Ecol*. 2010;24:776-784.
18. Grant P, Grant B. Adaptive radiation of Darwin's finches: recent data help explain how this famous group of Galapagos birds evolved, although gaps in our understanding remain. *Am Sci*. 2002;90:130.
19. Freeman PW. Functional cranial analysis of large animalivorous bats (Microchiroptera). *Biol J Linn Soc*. 1984;21:387-408.
20. Santana SE, Dumont ER. Connecting behaviour and performance: the evolution of biting behaviour and bite performance in bats. *J Evol Biol*. 2009;22:2131-2145.
21. Dumont ER. Cranial shape in fruit, nectar, and exudate feeders: implications for interpreting the fossil record. *Am J Phys Anthropol*. 1997;102:187-202.
22. Santana SE, Grosse IR, Dumont ER. Dietary hardness, loading behavior, and the evolution of skull form in bats. *Evolution (N Y)*. 2012;66:2587-2598.
23. Mallarino R, Abzhanov A. Paths less traveled: Evo-Devo approaches to investigating animal morphological evolution. *Annu Rev Cell Dev Biol*. 2012;28:743-763.
24. Bhullar BAS, Marugán-Lobón J, Racimo F, Bever GS, Rowe TB, Norell MA, Abzhanov A. Birds have paedomorphic dinosaur skulls. *Nature*. 2012;487:223-226.
25. Koyabu D, Son NT. Patterns of postcranial ossification and sequence heterochrony in bats: life histories and developmental trade-offs. *J Exp Zool B Mol Dev Evol*. 2014;322(8):607-618.

26. Lieberman DE, McBratney BM, Krovitz G. The evolution and development of cranial form in *Homo sapiens*. *Proc Natl Acad Sci U S A*. 2002;99:1134-1139.
27. Mitteroecker P, Gunz P, Bernhard M, Schaefer K, Bookstein FL. Comparison of cranial ontogenetic trajectories among great apes and humans. *J Hum Evol*. 2004;46:679-698.
28. Morris ZS, Vliet KA, Abzhanov A, Pierce SE. Heterochronic shifts and conserved embryonic shape underlie crocodylian craniofacial disparity and convergence. *Proc R Soc B*. 2019;286: 20182389.
29. Piras P, Salvi D, Ferrara G, et al. The role of post-natal ontogeny in the evolution of phenotypic diversity in Podarcis lizards. *J Evol Biol*. 2011;24:2705-2720.
30. Da Silva FO, Fabre A-C, Savriama Y, et al. The ecological origins of snakes as revealed by skull evolution. *Nat Commun*. 2018; 9:376.
31. Bhullar BAS, Morris ZS, Sefton EM, et al. A molecular mechanism for the origin of a key evolutionary innovation, the bird beak and palate, revealed by an integrative approach to major transitions in vertebrate history. *Evolution (N Y)*. 2015;69:1665-1677.
32. Sanger TJ, Seav SM, Tokita M, et al. The oestrogen pathway underlies the evolution of exaggerated male cranial shapes in Anolis lizards. *Proc Biol Sci*. 2014;281:20140329.
33. Futuyma D. *Evolutionary Biology*. 2nd ed. Sunderland, MA: Sinauer Associates; 1986.
34. Gunter HM, Koppermann C, Meyer A. Revisiting de Beer's textbook example of heterochrony and jaw elongation in fish: calmodulin expression reflects heterochronic growth, and underlies morphological innovation in the jaws of belonoid fishes. *EvoDevo*. 2014;5:8.
35. Alberch P, Gould SJ, Oster GF, Wake DB. Size and shape in ontogeny and phylogeny. *Paleobiology*. 1979;5:296-317.
36. Albertson RC, Yan YL, Titus TA, et al. Molecular pedomorphism underlies craniofacial skeletal evolution in Antarctic notothenioid fishes. *BMC Evol Biol*. 2010;10:4.
37. Hall BK, Olson WM. Keywords and concepts in evolutionary developmental biology. *Harvard Univ Press Ref Libr:Xvi*. 2003; 476:343-361.
38. Gould SJ. *Ontogeny and Phylogeny*. Vol 28. Cambridge, MA: Harvard University Press; 1977:501.
39. Göbbel L. Morphology of the external nose in Hipposideros diadema and *Lavia frons* with comments on its diversity and evolution among leaf-nosed Microchiroptera. *Cells Tissues Organs*. 2002;170:39-60.
40. de Mello F, Hubbe M. Craniometric diversity of the common vampire bat (*Desmodus rotundus*) in Central and South America. *J Mammal*. 2012;93:579-588.
41. Muchhala N. Nectar bat stows huge tongue in its rib cage. *Nature*. 2006;444:701-702.
42. Peterson RL, Kirmse P. Notes on *Vampyrum spectrum*, the false vampire bat, in Panama. *Can J Zool*. 1969;47:140-142.
43. Cretekos CJ, Weatherbee SD, Chen CH, et al. Embryonic staging system for the short-tailed fruit bat, *Carollia perspicillata*, a model organism for the mammalian order Chiroptera, based upon timed pregnancies in captive-bred animals. *Dev Dyn*. 2005;233:721-738.
44. Hayssen V, Tienhoven A Van, Van Tienhoven A. *Asdell's Patterns of Mammalian Reproduction: A Compendium of Species-Specific Data*. Ithaca, NY: Cornell University Press; 1993.
45. Hockman D, Mason MK, Jacobs DS, Illing N. The role of early development in mammalian limb diversification: A descriptive comparison of early limb development between the natal long-fingered bat (*Miniopterus natalensis*) and the mouse (*Mus musculus*). *Dev Dyn*. 2009;238:965-979.
46. Jones KE, Bielby J, Cardillo M, et al. PanTHERIA: a species-level database of life history, ecology, and geography of extant and recently extinct mammals. *Ecology*. 2009;90:2648-2648.
47. Ortega J, Castro-Arellano I. *Artibeus jamaicensis*. *Mamm Species*. 2001;662:1-9.
48. Wang Z, Han N, Racey PA, Ru B, He G. A comparative study of prenatal development in Miniopterus schreibersii fuliginosus, Hipposideros armiger and *H. pratti*. *BMC Dev Biol*. 2010;10:10.
49. Arthur W. *Evolution: A Developmental Approach*. Oxford, UK: John Wiley & Sons; 2010.
50. Ridley M. *Evolution*. 3rd ed. Malden, MA: Blackwell Publishing Ltd; 2004:786.
51. Datzmann T, von Helversen O, Mayer F. Evolution of nectarivory in phyllostomid bats (Phyllostomidae gray, 1825, Chiroptera: Mammalia). *BMC Evol Biol*. 2010;10:165.
52. Pedersen SC. Morphometric analysis of the Chiropteran skull with regard to mode of echolocation. *J Mammal*. 1998;79:91-103.
53. Pedersen SC, Müller R. Nasal-emission and nose leaves. In: Krauel JJ, Mccracken GF, eds. *Bat Evolution, Ecology, and Conservation*. New York: Springer; 2013:71-91.
54. Yohe LR, Velazco PM, Rojas D, Gerstner BE, Simmons NB, Dávalos LM. Bayesian hierarchical models suggest oldest known plant-visiting bat was omnivorous. *Biol Lett*. 2015;11:10718-10722.
55. Santana SE, Strait S, Dumont ER. The better to eat you with: functional correlates of tooth structure in bats. *Funct Ecol*. 2011b;25: 839-847.
56. Abzhanov A. Von Baer's law for the ages: lost and found principles of developmental evolution. *Trends Genet*. 2013;29:712-722.
57. Klingenberg CP. Heterochrony and allometry: the analysis of evolutionary change in ontogeny. *Biol Rev Camb Philos Soc*. 1998; 73:79-123.
58. Mallarino R, Campas O, Fritz JA, et al. Closely related bird species demonstrate flexibility between beak morphology and underlying developmental programs. *Proc Natl Acad Sci U S A*. 2012; 109:16222-16227.
59. Mallarino R, Grant PR, Grant BR, Herrel A, Kuo WP, Abzhanov A. Two developmental modules establish 3D beak-shape variation in Darwin's finches. *Proc Natl Acad Sci U S A*. 2011;108:4057-4062.
60. Sanger TJ, Mahler DL, Abzhanov A, Losos JB. Roles for modularity and constraint in the evolution of cranial diversity among anolis lizards. *Evolution (N. Y.)*. 2012;66:1525-1542.
61. Saele O, Silva N, Pittman K. Post-embryonic remodelling of neurocranial elements: a comparative study of normal versus abnormal eye migration in a flatfish, the Atlantic halibut. *J Anat*. 2006;209:31-41.
62. Sears K. Differences in growth generate the diverse palate shapes of New World leaf-nosed bats (Order Chiroptera, Family Phyllostomidae). *Evol Biol*. 2014;1:12-21.
63. Young NM, Hu D, Lainoff AJ, et al. Embryonic bauplans and the developmental origins of facial diversity and constraint. *Development*. 2014;141:1059-1063.
64. Zelditch M, Swiderski D, Sheets H. *Geometric Morphometrics for Biologists: A Primer*. Vol 59. Oxford, UK: Elsevier; 2012:457.
65. Agnarsson I, Zambrana-Torrelio CM, Flores-Saldana NP, May-Collado LJ. A time-calibrated species-level phylogeny of bats (Chiroptera, Mammalia). *PLoS Curr*. 2011;3:RRN1212.

66. Tsagkogeorga G, Parker J, Stupka E, Cotton JA, Rossiter SJ. Phylogenomic analyses elucidate the evolutionary relationships of bats. *Curr Biol*. 2013;23:2262-2267.
67. Santana SE, Cheung E. Go big or go fish: morphological specializations in carnivorous bats. *Proc R Soc B Biol Sci*. 2016;283:20160615.
68. Aguirre LF, Herrel A, Van Damme R, Matthysen E. The implications of food hardness for diet in bats. *Funct Ecol*. 2003;17:201-212.
69. Clare EL, Goerlitz HR, Drapeau VA, et al. Trophic niche flexibility in *Glossophaga soricina*: how a nectar seeker sneaks an insect snack. *Funct Ecol*. 2014;28:632-641.
70. Fleming TH, Hooper ET, Wilson DE, Hooper T. Three central American bat communities: structure, reproductive cycles, and movement patterns. *Ecology*. 1972;53:556-569.
71. Fleming TH. Opportunism versus specialization: the evolution of feeding strategies in frugivorous bats. In *Frugivores Seed Dispersal*. Heidelberg, Germany: Springer, Dordrecht; 1986;105-118.
72. Fleming TH, Heithaus ER. Seasonal foraging behavior of the frugivorous bat *Carollia perspicillata*. *J Mammal*. 1986;67:660-671.
73. Gonzalez-Terrazas TP, Medellin RA, Knornschild M, Tschapka M. Morphological Specialization Influences Nectar Extraction Efficiency of Sympatric Nectar-Feeding Bats. *J Exp Biol*. 2012;215(22):3989-3996.
74. Humphrey SR, Bonaccorso FJ, Zinn TL. Guild structure of surface-gleaning bats in Panama. *Ecology*. 1983;64:284-294.
75. Kunz TH, Diaz CA. Folivory in fruit-eating bats, with new evidence from *Artibeus jamaicensis* (Chiroptera: Phyllostomidae). *Biotropica*. 1995;27:106.
76. Santana S, Geipel I, Dumont E. All you can eat: high performance capacity and plasticity in the common big-eared bat, Micronycteris microtis (Chiroptera: Phyllostomidae). *PLoS One*. 2011a;6: e28584.
77. Mueller K, Kaufman A. *Volume Graphics 2001*. New York, NY: Springer Science & Business Media; 2001.
78. Klingenberg CP. MorphoJ: an integrated software package for geometric morphometrics. *Mol Ecol Resour*. 2011;11:353-357.
79. Developement Core Team R. R: A language and environment for statistical computing. *R Found Stat Comput*. 2015;1:409.
80. Drummond AJ, Suchard MA, Xie D, Rambaut A. Bayesian phylogenetics with BEAUti and the BEAST 1.7. *Mol Biol Evol*. 2012; 29:1969-1973.
81. Rambaut A, Drummond AJ. 2013. Tracer v1.6. http//tree.bio.ed.ac.uk/software/tracer/. Accessed December 2018.
82. Swofford DL, Begle DP. 1993. *PAUP: Phylogenetic Analysis Using Parsimony, Version 3.1*. Champaign, Illinois: Illinois Natural History Survey; 259.
83. Adams DC, Otárola-Castillo E. Geomorph: an r package for the collection and analysis of geometric morphometric shape data. *Methods Ecol Evol*. 2013;4:393-399.
84. Revell LJ. Phytools: an R package for phylogenetic comparative biology (and other things). *Methods Ecol Evol*. 2012;3:217-223.
85. Esquerré D, Sherratt E, Keogh JS. Evolution of extreme ontogenetic allometric diversity and heterochrony in pythons, a clade of giant and dwarf snakes. *Evolution (N. Y.)*. 2017;71:2829-2844.
86. Koyabu D, Werneburg I, Morimoto N, et al. Mammalian skull heterochrony reveals modular evolution and a link between cranial development and brain size. *Nat Commun*. 2014;5:3625.
87. Mitteroecker P, Gunz P, Bookstein FL. Heterochrony and geometric morphometrics: A comparison of cranial growth in *Pan paniscus* versus *Pan troglodytes*. *Evol Dev*. 2005;7:244-258.

SUPPORTING INFORMATION

Additional supporting information may be found online in the Supporting Information section at the end of this article.

How to cite this article: Camacho J, Heyde A, Bhullar B-AS, Haelewaters D, Simmons NB, Abzhanov A. Peramorphosis, an evolutionary developmental mechanism in neotropical bat skull diversity. *Developmental Dynamics*. 2019;1–15. https://doi.org/10.1002/dvdy.90